A Stabilized PAN-FeS_2 Cathode with an EC/DEC Liquid Electrolyte

Seoung-Bum Son, Thomas A. Yersak, Daniela Molina Piper, Seul Cham Kim, Chan Soon Kang, Jong Soo Cho, Soon-Sung Suh, Young-Ugk Kim, Kyu Hwan Oh, and Se-Hee Lee**

In this study we embed phase pure natural cubic-FeS_2 (pyrite) in a stabilized polyacrylonitrile (PAN) matrix. The PAN matrix confines FeS_2's electroactive species (Fe^0 and S_n^{2-}) for good reversibility and efficiency. Additionally, the stabilized PAN matrix can accommodate the 160% volume expansion of FeS_2 upon full discharge because it is not fully carbonized. At room temperature, our PAN-FeS_2 electrode delivers a specific capacity of 470 mAh g^{-1} on its 50th discharge. Using high-resolution transmission electron microscopy (HRTEM) we confirm that FeS_2 particles are embedded in the PAN matrix and that FeS_2's mobile electroactive species are confined during cycling. We also observe the formation of orthorhombic-FeS_2 at full charge, which validates the results of our previous all-solid-state FeS_2 battery study.

The energy density of conventional Li-ion batteries with $LiMO_2$ (M = transition metal) cathodes and graphitic anodes is approaching a practical upper limit after two decades of optimization. In order to improve the energy density of Li-ion batteries further, new cathodes must be developed with capacities that compare to those of advanced anodes such as Si.[1] The FeS_2 conversion chemistry is a promising candidate to replace the $LiMO_2$ intercalation chemistry because FeS_2 is inexpensive, energy dense, and environmentally benign. The four electron reduction of cubic-FeS_2 (pyrite) with lithium ($FeS_2 + 4Li^+ + 4e^- \rightarrow Fe + 2Li_2S$) provides a specific capacity of 894 mAh g^{-1}, whereas, the very best $LiMO_2$ intercalation cathodes can only provide 200 mAh g^{-1}.[2–4] For these reasons Energizer popularized the FeS_2/Li chemistry as a primary battery,[5] but a secondary FeS_2/Li battery is not yet commercially available. The safety issues associated with lithium metal anodes can be cited as one obstacle obstructing the realization of a rechargeable FeS_2/Li battery,[6] however, the FeS_2 cathode also presents very difficult problems. This paper addresses the problems of the cathode by embedding natural pyrite in a commercially available, stabilized PAN matrix.

The problems associated with a rechargeable FeS_2 cathode can be understood by considering the electroactive species of FeS_2 during cycling. Though still the subject of much debate, a proposed reaction mechanism for cubic-FeS_2 at low temperatures is provided below for an initial discharge and subsequent charge.[3,7,8] From Equation (2) we see that small aggregates of superparamagnetic Fe^0 atoms are one product of the reduction of FeS_2 with four Li^+. Fe^0 particles have an average diameter of 3.6 nm and are highly reactive in order to catalyze the oxidation of the other full discharge product, Li_2S, which is highly resistive. Unfortunately, nano-Fe^0 particles tend to agglomerate into non-reactive α-Fe particles which results in the electrochemical isolation of Li_2S and a rapid loss of battery capacity.[7,9]

From Equation (5) it is also evident that cubic-FeS_2 is not reformed at full charge. Our previous work found that the charge products of an all-solid-state cubic-FeS_2 cathode are a multiphase mixture of ortho-FeS_2 (marcasite), $FeS_{8/7}$, and S.[7] Prior to this study it was generally accepted that the charge products were only $Fe_{1-x}S$ and S from the disproportionation of an $Li_{2-x}FeS_2$ intermediary phase.[3] This work will provide further evidence that ortho-FeS_2 is a charge product at ambient temperature. More importantly, the reversibility and efficiency of FeS_2 batteries will suffer from the same problems as that of a Li-S battery because sulfur is one of the three proposed charge products. The initial reduction of sulfur produces soluble and highly mobile polysulfides (S_n^{2-}). The dissolution of these polysulfides into an organic liquid electrolyte contributes to capacity fade and results in a parasitic redox shuttle that reduces charging efficiency.[10–12]

Initial Discharge

$$FeS_2 + 2Li^+ + 2e^- \rightarrow Li_2FeS_2 \quad (1)$$

$$Li_2FeS_2 + 2Li^+ + 2e^- \rightarrow Fe^0 + 2Li_2S \quad (2)$$

Subsequent Charge

$$Fe^0 + 2Li_2S \rightarrow Li_2FeS_2 + 2Li^+ + 2e^- \quad (3)$$

$$Li_2FeS_2 \rightarrow Li_{2-x}FeS_2 + xLi_+ + xe^- (0.5 < x < 0.8) \quad (4)$$

S.-B. Son, S. C. Kim, C. S. Kang, Prof. K. H. Oh
Department of Materials Science and Engineering
Seoul National University
Seoul, 151–742, Korea
E-mail: kyuhwan@snu.ac.kr
T. A. Yersak, D. M. Piper, J. S. Cho, Prof. S.-H. Lee
Department of Mechanical Engineering
University of Colorado at Boulder
Boulder, CO, 80309, USA
E-mail: sehee.lee@colorado.edu
J. S. Cho
MK electron
316–2 Geumeo-ri, Pogok-myeon, Yongin-si
Gyeong gi-do, 449–810, Korea
S.-S. Suh, Y.-U. Kim
Samsung SDI Co. Ltd.
Giheung-gu, Yongin-si, Gyeonggi-do, 446–577, Korea

DOI: 10.1002/aenm.201300961

$$Li_{2-x}FeS_2 \rightarrow 0.8\,\text{ortho-}FeS_2 + 0.2FeS_{8/7} + 0.175S + (2-x)Li^+ + (2-x)e^- \quad (5)$$

The mobility of Fe^0 and polysulfides in organic liquid electrolytes explains why conventional FeS_2 cathodes are not reversible. An all-solid-state battery architecture is uniquely capable of confining the electroactive species of FeS_2[9,13] and we recently demonstrated the full reversibility of FeS_2 as a cathode versus lithium metal at 60 °C.[7] Although this study represents a milestone for the secondary FeS_2 conversion chemistry, it is still more desirable to incorporate FeS_2 into a conventional liquid or polymer battery because the manufacturing processes associated with conventional batteries are mature. Prior to our work, many studies attempted to use composite polymer electrolytes to confine FeS_2's electroactive species.[4,14] Unfortunately, none of these studies could demonstrate acceptable reversibility because polymer electrolytes do not provide sufficient confinement. More recently, other studies have examined the cycle ability of synthetic FeS_2/carbon and FeS_2/PANI composites in liquid electrolytes with limited success.[4,11,15,16]

Here, we embed FeS_2 in a stabilized PAN matrix that confines electroactive species to prevent active material loss and improve Coulombic efficiency (CE). Stabilized PAN enables the reversibility of FeS_2 by considering the need to not only confine FeS_2's electroactive species but also to accommodate FeS_2's expansion. The effectiveness of stabilized polymers as confining matrices has been previously demonstrated with PAN-S and PANi-S composites.[17,18] It has also been shown that thin coatings of stabilized PAN can accommodate the 300% volume expansion of nano-Si particles.[19] By avoiding the full carbonization of PAN the elastic properties of the PAN precursor can be retained, while the conjugation of PAN during the stabilization process provides good electronic conductivity.[20] More importantly, the preparation of the PAN-FeS_2 composite is simple and the precursors are inexpensive, commercially available natural pyrite and PAN. The results of this study will demonstrate that the challenges associated with a conventional FeS_2 cathode can be overcome.

Figure 1 presents the microstructure and elemental mapping of an uncycled PAN-FeS_2 composite electrode. A focused ion beam (FIB) microscope was used to prepare a sample for high-resolution transmission electron microscopy (HRTEM). Platinum was deposited on the electrode surface in order to protect the observation area during FIB cross sectioning. For a more detailed description of the TEM specimen preparation process please refer to Supporting Information Figure S3 and our previous work.[21] A cross-sectional image (Figure 1a) shows that most ball milled FeS_2 particles are fully embedded in the stabilized PAN matrix. Figure 1b presents the electron energy loss spectrum (EELS) zero-loss image and Figure 1c presents the EELS elemental mapping of the same cross-sectioned sample. EELS mapping shows that the PAN matrix area is matched with C (red) and the embedded particles are matched with Fe (blue) and S (green).

Two electrodes were characterized electrochemically using a constant current, constant voltage (CCCV) cycling protocol. The first electrode was made with the PAN-FeS_2 electrode material presented in Figure 1 while the second electrode is a control sample, which we call bare FeS_2. Both cells were cycled

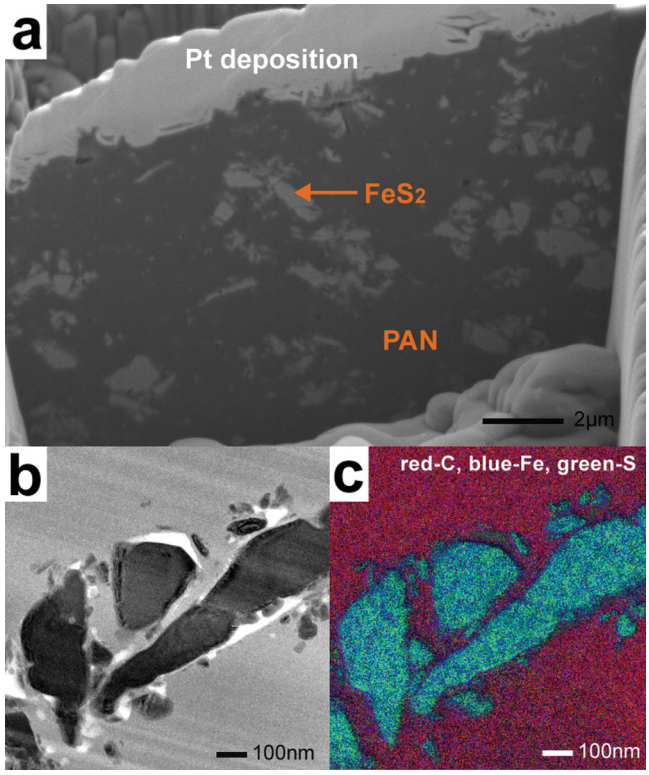

Figure 1. a) Cross-sectional SEM image of an uncycled PAN-FeS_2 electrode. b) TEM image with EELS zero-loss mode of the stabilized PAN matrix (light) and embedded FeS_2 particles (dark). c) EELS elemental mapping of C (red), Fe (blue), and S (green).

between 1 V and 3 V at a rate of 0.1 C for all cycles. The cyclic stabilities and CE of the PAN-FeS_2 (red) and bare FeS_2 (orange) electrodes are provided in **Figure 2**a. Bare FeS_2 delivers an initial discharge capacity of 828 mAh g^{-1}, which is close to FeS_2's theoretical capacity of 894 mAh g^{-1}. Bare FeS_2 has a notably low initial CE of 63% along with a consistently low cycling CE, drastically hindering its capacity retention so that by the 20th cycle it delivers a discharge capacity of only 120 mAh g^{-1}, or only 14% of its initial discharge capacity. Though PAN-FeS_2 delivers a lower initial discharge capacity of 729 mAh g^{-1}, its cyclic stability and CE are greatly improved compared to bare FeS_2. With a significantly improved initial CE of 94%, our PAN-FeS_2 electrode delivers 470 mAh g^{-1}, a discharge capacity retention value of 64%, with a CE approaching 99.25% by the 50th cycle. Other FeS_2-C composite electrodes showed at most ≈350 mAh g^{-1} by the 40th cycle.[4,15] PAN-FeS_2 not only exceeds capacities shown by previous work, but it is also unique in that the precursors are commercially available natural pyrite and PAN.[4,14] Figure 2b,c provide the voltage profiles for PAN-FeS_2 and bare FeS_2, respectively. The stable capacity of PAN-FeS_2 is correlated with voltage profiles that are more stable compared to that of bare FeS_2. With cycling, bare FeS_2's voltage profiles develop overpotentials and lose the upper charging voltage plateau at approximately 2.4 V.

To better understand the mechanism behind the improved stability of the PAN-FeS_2 electrode and identify the phases present at full charge, we use TEM and EELS to study the

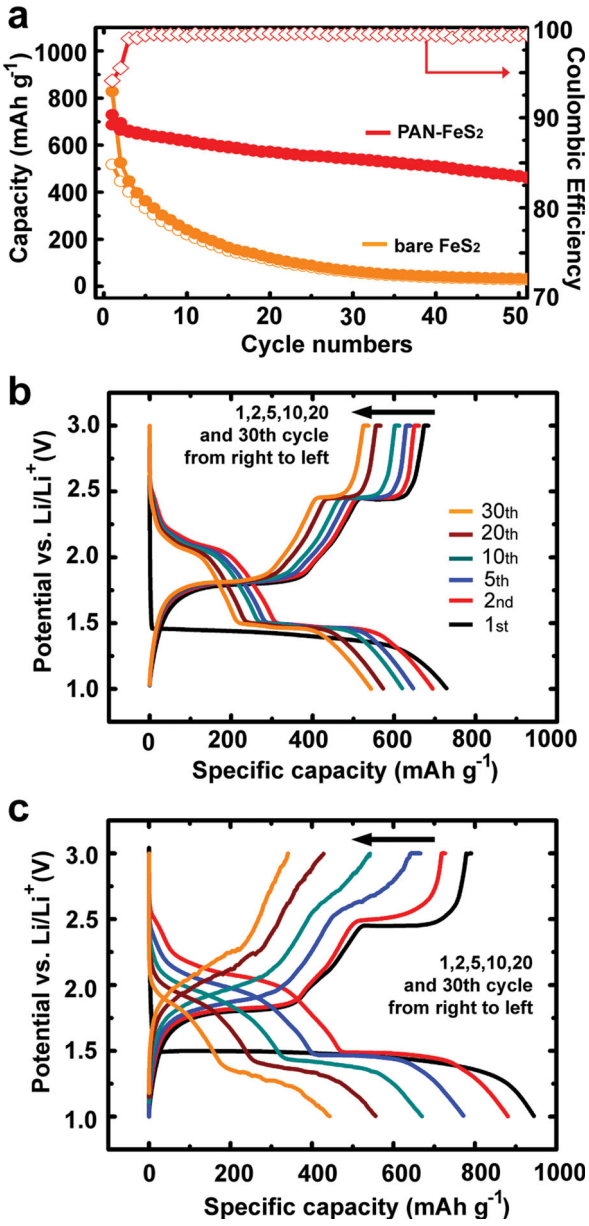

Figure 2. a) Cyclic stability of the stabilized PAN-FeS_2 electrode versus that of a bare FeS_2 electrode. Specific capacity is reported with respect to the mass of the FeS_2 active material. b) Voltage profiles of PAN-FeS_2. c) Voltage profiles of bare FeS_2.

microstructure of a PAN-FeS_2 electrode recovered after completion of its 10th charge. As with the uncycled PAN-FeS_2 sample, the 10th charge TEM sample is prepared using a FIB microscope (Supporting Information Figure S3). The bright field TEM image of an embedded FeS_2 particle is provide in **Figure 3**a while the HRTEM image and fast Fourier transform (FFT) of the same particle is provided in Figure 3b. Although we observed cubic-FeS_2 before cycling, the FFT of the HRTEM image matches with ortho-FeS_2 (marcasite) along the [01–1] zone axis. Because our electrode is made with phase pure natural cubic-FeS_2 (Supporting Information Figure 2b), we conclude that the observed ortho-FeS_2 is produced electrochemically. This result

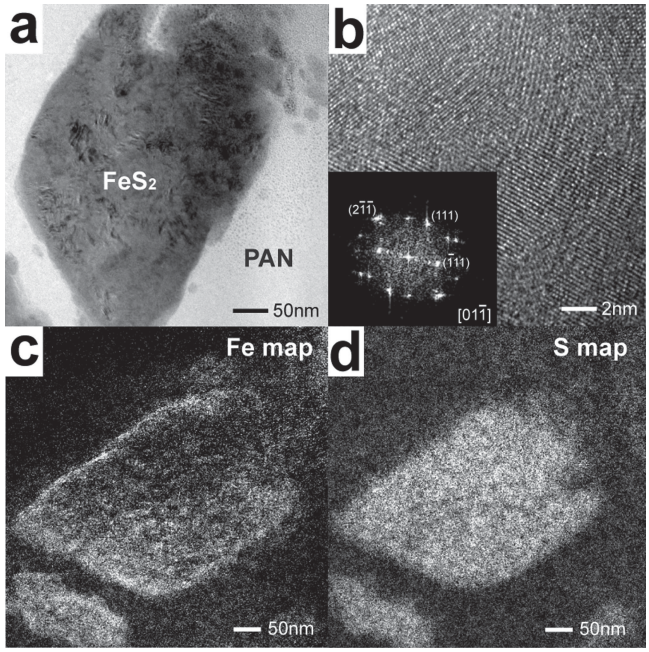

Figure 3. a) TEM image of an embedded FeS_2 particle in a PAN-FeS_2 electrode collected after completion of its 10th charge. b) High resolution (HR) image of the FeS_2 particle in panel (a) and the corresponding FFT pattern matched with orthorhombic-FeS_2 along the [01–1] zone axis. c) EELS elemental mapping for Fe. d) EELS elemental mapping of S.

is consistent with our previous all-solid-state FeS_2/Li battery study where we observed ortho-FeS_2 as a charge product.[7] It is the first time that ortho-FeS_2 has been observed in an ambient temperature battery because the aforementioned all-solid-state FeS_2 sample was recovered after charging at 60 °C. Later in the discussion we will analyze the differential capacities (dQ/dV) of the two electrodes presented in Figure 2 in order to provide further evidence that Equation (5) is the valid reaction for FeS_2's final charging step.

Figure 3c,d display the EELS elemental mapping of Fe and S while Supporting Information Figure S5 shows the zero-loss and the EELS mapping of C for the same particle. After cycling, it is clear that there is no migration of S or Fe into the stabilized PAN matrix. This result suggests that the stabilized PAN matrix completely obstructs the dissolution of intermediate polysulfides into the liquid electrolyte and prevents the reaction of Fe^0 with the liquid electrolyte. Confinement of polysulfides explains why PAN-FeS_2 exhibited a higher CE than bare FeS_2. By confining polysulfides in PAN the parasitic shuttle mechanism, which reduces charging efficiency, cannot be initiated. It also suggests that our stabilized PAN is not very porous to accommodate the passage of solvated polysulfides. Supporting this idea, we measured the Brunauer-Emmett-Teller (BET) porosity of PAN-FeS_2 to be only 1.50 $m^2\ g^{-1}$. Because PAN-FeS_2 has such a low porosity, it also suggests that it is difficult for the liquid electrolyte to impregnate the stabilized PAN matrix. Previously, we have found that stabilized PAN is electrochemically active and stable against the liquid electrolyte between 50 mV and 1 V.[19] Here, we also show PAN's electrochemical stability within a voltage window of 1 V to 3 V after running parallel experiments to those

reported in this work with cells only containing stabilized PAN and no FeS_2 (Supporting Information Figure S6). We suspect that stabilized PAN is a mixed conductor, however, more work is currently underway to characterize its conductive properties.

We have shown that elemental S and Fe are not observed in our stabilized PAN matrix after cycling which verifies the complete confinement of FeS_2's intermediary electroactive species. However, we still observe some capacity fade. To explain this, some FeS_2 particles are not fully embedded within our stabilized PAN matrix during material preparation so they are subject to attack by the liquid electrolyte during cycling. To fully coat every particle, we propose a direct electrode blading with stabilized PAN as previously described.[19] In this way, partially embedded FeS_2 particles will be protected by a secondary protective coating of stabilized PAN.

As stated earlier, FeS_y and S were generally believed to be the final charge products of a low temperature FeS_2 battery.[3] Reductive dQ/dV analysis in the range of 2.0 V to 2.8 V (**Figure 4**) can be used to differentiate the direct reduction

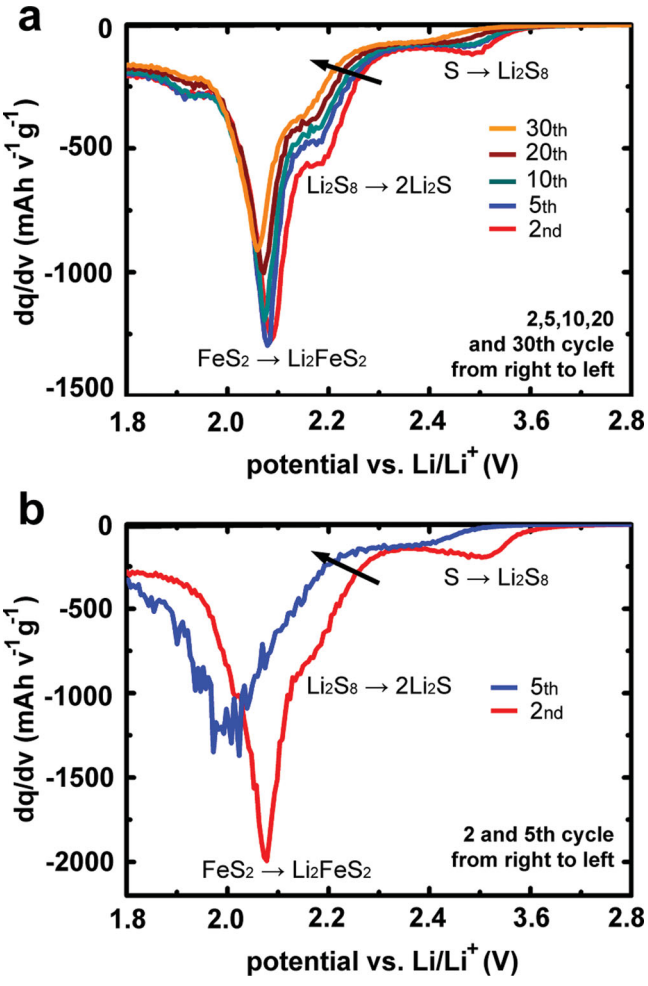

Figure 4. a) Reductive dQ/dV profiles for the PAN-FeS_2 electrode and b) reductive dQ/dV profiles for the bare FeS_2 electrode. The peaks at approximately 2.5 V and 2.2 V are attributed to Equation (6) and Equations (7) and (8), respectively, while the peak at approximately 2.1 V is attributed to Equation (1).

of S from the reduction of ortho-FeS_2 and lend further support to the validity of Equation (5). Supporting Figure S7 provides the dQ/dV for both PAN-FeS_2 and bare FeS_2 in the whole voltage range of 1 V to 3 V. As expected we observe three peaks in the range 2.0 to 2.5 V: one for ortho-FeS_2 (2.1 V) and two for sulfur (2.2 V and 2.5 V). The peak at 2.5 V is not a side reaction because if it were it would have also been observed during the initial discharge, however, because sulfur was not yet present the peak is also not present. The peak at 2.1 V corresponds to the reduction of ortho-FeS_2 to Li_2FeS_2 (Equation (1)), whereas the peaks at 2.5 and 2.2 V correspond to the reduction of S (Equations (6), (7), and (8)). During the initial discharge the reduction of cubic-FeS_2 occurs at 1.5–1.7 V, while on subsequent cycles the reduction of ortho-FeS_2 occurs at 2.1 V. The explanation for the difference may be related to a change in microstructure or kinetics.[7]

In a liquid cell the direct reduction of sulfur occurs in two steps even though the thermodynamic phase diagram suggests only one plateau. The reduction of S follows a three step process as presented below.[12] The first step, Equation (6), occurs at a higher voltage than the other two steps because the mobility and molecular nature of the polysulfides improves the reaction kinetics. Sulfur does not exhibit two plateaus in an all-solid-state structure because polysulfides are confined such that their reduction does not enjoy a kinetic advantage. The presence of two sulfur plateaus for PAN-FeS_2 suggests that some polysulfides are mobile in the liquid electrolyte and that the confinement of FeS_2 is incomplete. This corroborates our previous observation that some FeS_2 particles are not fully embedded in the PAN matrix.

$$S_8 + 4Li^+ + 4e^- \rightarrow 2Li_2S_4 \quad (6)$$

$$Li_2S_4 + 2Li^+ + 2e^- \rightarrow Li_2S_2 \downarrow \quad (7)$$

$$Li_2S_2 + 2Li^+ + 2e^- \rightarrow 2Li_2S \quad (8)$$

In summary, the performance of the PAN-FeS_2 composite cathode suggests that the problems associated with the mobility of FeS_2's electroactive species can be addressed without the need for a costly all-solid-state battery structure. By the 50th cycle our PAN-FeS_2 electrode delivers 470 mAh g^{-1}, or 64% of its initial discharge capacity with a CE approaching 99.25%. When viewed alongside a recent development regarding dendrite-free lithium metal anodes,[22] the results of our stabilized PAN-FeS_2 cathode study suggest that a practical, safe conventional secondary FeS_2/Li battery is close to reality. Moreover, we also observed ortho-FeS_2 (marcasite) as a full charge product which is a first for conventional liquid batteries and validates the results of our previous all-solid-state FeS_2 battery study.

Experimental Section

First, naturally occurring pyrite (FeS_2, Alfa Aesar) was mechanically ground at 400 rotations per minute (RPM) for 1 h using a planetary ball mill (Across International) in order to reduce the average particle size. Next, ball milled FeS_2 and PAN (MW = 150 000 g mol^{-1}, Sigma Aldrich) were mixed in a mass ratio of 7:3, respectively, using a mortar and pestle. The mixture was then dissolved in *N*,*N*-dimethylformamide

(DMF, 99%, Alfa Aesar), stirred via magnetic stirring for 6 h, and then dried overnight. The stabilization of PAN followed a two-step process. The dried PAN-FeS_2 mixture was first heat treated in air at 200 °C for 1 h (Thermolyne) and then heat treated under Ar flow at 500 °C for 1 h (Thermo Scientific). The heating and cooling rate for each heat treatment was 1.66 °C per min.[20]

A cathode slurry was prepared by combining PAN-FeS_2, acetylene black (Alfa Aesar), and PVDF (poly (vinylidene floride), Alfa Aesar) binder in a 60:20:20 weight ratio, respectively, with a 1-methyl-2-pyrrolidinone (NMP, Alfa Aesar) solvent. The slurry was coated on Al foil, dried under air, and then calendared. On average, the FeS_2 active material loading is 1.5 mg cm^{-2}, and the area of each of the tested electrodes was of 1.33 cm^2. Test coin cells (2032, Pred Materials) were assembled with the prepared PAN-FeS_2 working electrode, a lithium metal foil counter electrode (Alfa Aesar), a glass fiber separator (Whatman, GF/G), and 1.5 M $LiPF_6$ in ethylene carbonate, diethyl carbonate (50:50, Soulbrain) electrolyte. The test cells were cycled using a constant current, constant voltage (CCCV) testing protocol between the voltage range of 1 V and 3 V at a constant rate of 0.1C. The voltage is held constant at 3 V at the end of each charging cycle for 30 min.

The microstructure of PAN-FeS_2 structure was investigated by analytical TEM (TECNAI F20 equipped with EELS) operating at 200 keV. As previously described, the TEM samples were prepared by sectioning a cycled electrode using a FIB's Ga^+ beam (FEI, NOVA200 dual beam system).[23]

Supporting Information

Supporting Information is available from the Wiley Online Library or from the author.

Acknowledgements

This work was supported by the National Science Foundation (NSF, CHE-1231048). Work at Seoul National University was supported by a grant from the Fundamental R&D Program for Technology of World Premier Materials funded by the Ministry of Knowledge Economy, Republic of Korea (10037919), a grant from the Center for Iron and Steel Research Institute of Advanced Materials (RIAM, D-BB04–11, 0417–20110105).

Received: August 2, 2013
Revised: August 26, 2013
Published online: October 11, 2013

[1] U. Kasavajjula, C. Wang, A. J. Appleby, *J. Power Sources* **2007**, *163*, 1003.

[2] a) Z. Tomczuk, B. Tani, N. C. Otto, M. F. Roche, D. R. Vissers, *J. Electrochem. Soc.* **1982**, *129*, 925; b) D. Bernardi, J. Newman, *J. Electrochem. Soc.* **1987**, *134*, 1309; c) J. Cabana, L. Monconduit, D. Larcher, M. R. Palacin, *Adv. Mater.* **2010**, *22*, E170; d) M. S. Whittingham, *Chem. Rev.* **2004**, *104*, 4271; e) J. B. Goodenough, *J. Power Sources* **2007**, *174*, 996.

[3] R. Fong, J. R. Dahn, C. H. W. Jones, *J. Electrochem. Soc.* **1989**, *136*, 3206.

[4] Y. J. Choi, N. W. Kim, K. W. Kim, K. K. Cho, G. B. Cho, H. J. Ahn, J. H. Ahn, K. S. Ryu, H. B. Gu, *J. Alloys Compd.* **2009**, *485*, 462.

[5] Y. Shao-Horn, S. Osmialowski, Q. C. Horn, *J. Electrochem. Soc.* **2002**, *149*, A1499.

[6] D. Aurbach, E. Zinigrad, Y. Cohen, H. Teller, *Solid State Ionics* **2002**, *148*, 405.

[7] T. A. Yersak, H. A. Macpherson, S. C. Kim, V. D. Le, C. S. Kang, S. B. Son, Y. H. Kim, J. E. Trevey, K. H. Oh, C. Stoldt, S. H. Lee, *Adv. Energy Mater.* **2013**, *3*, 120.

[8] a) R. Brec, A. Dugast, A. Le Mehauté, *Mater. Res. Bull.* **1980**, *15*, 619; b) D. Golodnitsky, E. Peled, *Electrochim. Acta* **1999**, *45*, 335; c) C. H. W. Jones, P. E. Kovacs, R. D. Sharma, R. S. Mcmillan, *J. Phys. Chem.* **1991**, *95*, 774.

[9] K. Takada, Y. Kitami, T. Inada, A. Kajiyama, M. Kouguchi, S. Kondo, M. Watanabe, M. Tabuchi, *J. Electrochem. Soc.* **2001**, *148*, A1085.

[10] a) R. D. Rauh, F. S. Shuker, J. M. Marston, S. B. Brummer, *J. Inorg. Nucl. Chem.* **1977**, *39*, 1761; b) R. D. Rauh, K. M. Abraham, G. F. Pearson, J. K. Surprenant, S. B. Brummer, *J. Electrochem. Soc.* **1979**, *126*, 523; c) B. L. Ellis, K. T. Lee, L. F. Nazar, *Chem. Mater.* **2010**, *22*, 691.

[11] X. L. Ji, K. T. Lee, L. F. Nazar, *Nat. Mater.* **2009**, *8*, 500.

[12] X. L. Ji, L. F. Nazar, *J. Mater. Chem.* **2010**, *20*, 9821.

[13] K. Takada, K. Iwamoto, S. Kondo, *Solid State Ionics* **1999**, *117*, 273.

[14] a) S. Y. Huang, X. Y. Liu, Q. Y. Li, J. Chen, *J. Alloys Compd.* **2009**, *472*, L9; b) E. Peled, D. Golodnitsky, G. Ardel, J. Lang, Y. Lavi, *J. Power Sources* **1995**, *54*, 496; c) E. Strauss, D. Golodnitsky, K. Freedman, A. Milner, E. Peled, *J. Power Sources* **2003**, *115*, 323; d) E. Strauss, D. Golodnitsky, E. Peled, *Electrochim. Acta* **2000**, *45*, 1519.

[15] a) D. Zhang, X. L. Wang, Y. J. Mai, X. H. Xia, C. D. Gu, J. P. Tu, *J. Appl. Electrochem.* **2012**, *42*, 263; b) D. Zhang, Y. J. Mai, J. Y. Xiang, X. H. Xia, Y. Q. Qiao, J. P. Tu, *J. Power Sources* **2012**, *217*, 229.

[16] D. Zhang, J. P. Tu, Y. J. Mai, J. Zhang, Y. Q. Qiao, X. L. Wang, *J. Aust. Ceram. Soc.* **2012**, *48*, 189.

[17] J. Fanous, M. Wegner, J. Grimminger, A. Andresen, M. R. Buchmeiser, *Chem. Mater.* **2011**, *23*, 5024.

[18] a) C. Wang, T. Sakai, O. Watanabe, K. Hirahara, T. Nakanishi, *J. Electrochem. Soc.* **2003**, *150*, A1166; b) X. G. Yu, J. Y. Xie, J. Yang, H. J. Huang, K. Wang, Z. S. Wen, *J. Electroanal. Chem.* **2004**, *573*, 121.

[19] D. M. Piper, T. A. Yersak, S. B. Son, S. C. Kim, C. S. Kang, K. H. Oh, C. M. Ban, A. C. Dillon, S. H. Lee, *Adv. Energy Mater.* **2013**, *3*, 697.

[20] M. S. A. Rahaman, A. F. Ismail, A. Mustafa, *Polym. Degrad. Stabil.* **2007**, *92*, 1421.

[21] S.-B. Son, S. C. Kim, C. S. Kang, T. A. Yersak, Y.-C. Kim, C.-G. Lee, S.-H. Moon, J. S. Cho, J.-T. Moon, K. H. Oh, S.-H. Lee, *Adv. Energy Mater.* **2012**, *2*, 1226.

[22] F. Ding, W. Xu, G. L. Graff, J. Zhang, M. L. Sushko, X. Chen, Y. Shao, M. H. Engelhard, Z. Nie, J. Xiao, *J. Am. Chem. Soc.* **2013**, *135*, 4450.

[23] S. B. Son, J. E. Trevey, H. Roh, S. H. Kim, K. B. Kim, J. S. Cho, J. T. Moon, C. M. DeLuca, K. K. Maute, M. L. Dunn, H. N. Han, K. H. Oh, S. H. Lee, *Adv. Energy Mater.* **2011**, *1*, 1199.

[24] I. C. Hoare, H. J. Hurst, W. I. Stuart, T. J. White, *J. Chem. Soc.-Faraday Trans. I* **1988**, *84*, 3071.

[25] J. Guo, Z. Yang, Y. Yu, H. c. D. Abruña, L. A. Archer, *J. Am. Chem. Soc.* **2012**, *135*, 763.

